



Published in final edited form as:

Nat Commun. 2014 ; 5: 3315. doi:10.1038/ncomms4315.

A Functional Interaction between Hippo-YAP Signaling and FoxO1 Mediates the Oxidative Stress Response

Dan Shao¹, Peiyong Zhai¹, Dominic P. Del Re¹, Sebastiano Sciarretta¹, Norikazu Yabuta², Hiroshi Nojima², Dae-Sik Lim³, Duoja Pan⁴, and Junichi Sadoshima^{1,*}

¹Department of Cell Biology and Molecular Medicine, Cardiovascular Research Institute, New Jersey Medical School, Rutgers Biomedical and Health Sciences, Newark, New Jersey 07103, USA

²Department of Molecular Genetics, Research Institute for Microbial Diseases, Osaka University, Suita, Osaka 565-0871, Japan

³Department of Biological Sciences, National Creative Research Initiatives Center, Biomedical Research Center, Graduate School of Medical Science and Engineering, Korea Advanced Institute of Science and Technology, Daejeon, 305-701, Korea

⁴Howard Hughes Medical Institute and Department of Molecular Biology and Genetics, Johns Hopkins University School of Medicine, Baltimore, Maryland 21218, USA

Abstract

The Hippo pathway is an evolutionarily conserved regulator of organ size and tumorigenesis that negatively regulates cell growth and survival. Here we report that YAP, the terminal effector of the Hippo pathway, interacts with FoxO1 in the nucleus of cardiomyocytes, thereby promoting survival. YAP and FoxO1 form a functional complex on the promoters of the catalase and MnSOD antioxidant genes and stimulate their transcription. Inactivation of YAP, induced by Hippo activation, suppresses FoxO1 activity and decreases antioxidant gene expression, suggesting that Hippo signaling modulates the FoxO1-mediated antioxidant response. In the setting of ischemia/reperfusion (I/R) in the heart, activation of Hippo antagonizes YAP-FoxO1, leading to enhanced oxidative stress-induced cell death through downregulation of catalase and MnSOD. Conversely, restoration of YAP activity protects against I/R injury. These results suggest

Users may view, print, copy, and download text and data-mine the content in such documents, for the purposes of academic research, subject always to the full Conditions of use:http://www.nature.com/authors/editorial_policies/license.html#terms

*Correspondence: Junichi Sadoshima, MD PhD, Department of Cell Biology and Molecular Medicine, New Jersey Medical School, Rutgers Biomedical and Health Sciences, 185 South Orange Ave., MSB G609, Newark, NJ 07103, Tel: 973-972-8619, Fax: 973-972-8919, sadoshju@njms.rutgers.edu.

Supplementary Information

Supplementary information includes nine figures.

Author Contributions

D.S. carried out experimental work, analyzed data and wrote the manuscript. P.Z. performed the mouse heart I/R surgery. D.D. studied the I/R phenotype of Lats2-CKO mice. S.S. performed the X-GAL staining for the mouse heart. N.Y. and H.N. generated p-Lats2 antibodies. J.S. supervised the research and corrected the manuscript. All authors contributed to editing the manuscript.

Competing financial interests

The authors declare no competing financial interests.

that YAP is a nuclear co-factor of FoxO1 and that the Hippo pathway negatively affects cardiomyocyte survival by inhibiting the function of YAP-FoxO1.

Introduction

Originally identified in *Drosophila melanogaster*, the Hippo pathway is an evolutionarily conserved regulator of organ size that controls both cell proliferation and apoptosis¹. The key components of the mammalian Hippo pathway include sterile 20-like kinases (Mst1 and Mst2; homologs of *Drosophila hippo*), the large tumor suppressors (Lats1 and Lats2; homologs of *warts*), and Yes-associated protein (YAP) and its paralog protein Transcriptional co-activator with PDZ-binding motif (TAZ), transcriptional co-activators and homologs of *yorkie*. YAP/TAZ regulates transcription of TEAD, p73, and Runx2 in the nucleus, thereby controlling growth and death in many cell types¹. Activation of Lats1/2 by Mst1/2 induces phosphorylation and nuclear exit/proteolytic degradation of YAP/TAZ, thereby negatively regulating YAP/TAZ.

Increasing lines of evidence suggest that inactivation of the Hippo pathway leads to uncontrolled cell proliferation in epithelial cells and stem cells^{2,3} and oncogenic transformation⁴⁻⁶, both of which are mediated through hyperactivity of YAP^{2,3}. Hippo signaling and its regulation of YAP modulate heart size by restraining cardiomyocyte proliferation during fetal development^{7,8}. Recent evidence suggests that activation of YAP also promotes myocardial regeneration after myocardial infarction (MI) by promoting proliferation of cardiomyocytes in adult hearts⁹, while activation of the Hippo components, including Mst1 and/or Lats2, in the adult heart promotes cardiomyocyte apoptosis^{10,11}. Postnatal genetic deletion of YAP leads to cardiac dysfunction and premature death in mice¹², suggesting that the upstream Hippo pathway promotes cell death and that YAP promotes cell survival in post-mitotic hearts. It should be noted that the molecular mechanism through which YAP promotes cell survival in cardiomyocytes is unknown. Given that YAP acts as a transcriptional co-factor, it is important to identify the transcription factor(s) through which YAP promotes cardiomyocyte survival in postnatal hearts.

The Hippo signaling pathway plays an important role in mediating oxidative stress induced-cell death. For example, Mst1 mediates neuronal cell death in response to H₂O₂¹³. Ischemia/reperfusion (I/R), which is known to cause myocardial injury and cardiac dysfunction, induces enhanced production of reactive oxygen species (ROS) and cardiomyocyte death through Mst1-dependent mechanisms¹⁰. Interestingly, stimulation of YAP prevents, whereas downregulation of YAP promotes, H₂O₂-induced cardiomyocyte death¹², suggesting causative involvement of YAP in cardiomyocyte survival during oxidative stress. However, the molecular mechanism through which YAP mediates the survival of cardiomyocytes remains to be elucidated.

FoxO1 belongs to the family of transcription factors possessing a conserved DNA binding domain termed the "Forkhead box"¹⁴. FoxO1 plays a fundamental role in regulating cell cycle, apoptosis, atrophy, autophagy, and energy homeostasis^{14,15}. FoxO1 also mediates protective effects against oxidative stress through regulation of antioxidant genes, including catalase and MnSOD^{16,17}. Conditional deletion of FoxO1 in the heart increases cell death

and reduces cardiac function in response to MI, suggesting that FoxO1 promotes cardiomyocyte survival in response to oxidative stimuli¹⁸. However, the signaling cascade that regulates FoxO1 activity during I/R is not yet understood.

Here we show that YAP forms a functional complex with FoxO1 in mediating antioxidant gene expression in response to I/R in the heart. Activation of Hippo signaling inhibits the YAP-FoxO1 complex and promotes cell death in response to oxidative stress. Our results suggest that FoxO1 acts as a downstream effector of YAP to regulate cardiomyocyte survival.

Results

YAP functions as a transcriptional co-activator of FoxO1

We have shown previously that downregulation of YAP confers cellular hypersensitivity to ROS and induces cardiomyocyte death *in vitro*¹². Consistently, cardiac-specific deletion of YAP induced accumulation of ROS in the mouse heart (Supplementary Fig. 1a, b), suggesting that YAP is involved in redox homeostasis regulation. FoxO1 transcriptionally upregulates antioxidant genes in response to oxidative stress and prevents cell death^{16,17}. Given the fact that Hippo-YAP signaling mediates cell death in response to oxidative stress, we hypothesized that FoxO1 may functionally interact with the Hippo pathway.

We performed immunocytochemistry experiments and found that YAP and FoxO1 co-localized in the nucleus (Fig. 1a). Using the *in situ* proximity ligation assay, we also observed that endogenous YAP and FoxO1 physically interact with one another in the nuclei of neonatal cardiomyocytes *in vitro* and of adult cardiomyocytes in the mouse heart *in vivo* (Fig. 1b and Supplementary Fig. 2a). Co-immunoprecipitation assays confirmed that endogenous YAP associates with FoxO1 in cardiomyocytes (Fig. 1c), and GST pull-down assays revealed that YAP directly binds to FoxO1 (Fig. 1d). YAP dose-dependently stimulated FoxO1 transcriptional activity, as evaluated with a FoxO1-luciferase reporter gene (FoxO1-luc) driven by three canonical FoxO1 response elements (Fig. 1e). Taken together, these results suggest that YAP acts as a transcriptional co-activator of FoxO1. Since FoxO1 and FoxO3 have overlapping functions in the heart, we examined whether YAP also interacts with FoxO3. Co-immunoprecipitation assays showed that YAP was not associated with FoxO3 (Supplementary Fig. 2b), indicating isoform-specific interaction between YAP and FoxO1. We further examined which domain of YAP is essential for physical interaction with and transcriptional activation of FoxO1. Mutation of Ser⁹⁴ in the TEAD binding site to alanine (S94A) significantly reduced the interaction between YAP and FoxO1, and partially attenuated YAP-mediated FoxO1 activation (Supplementary Fig. 2c, d). Although N-terminal YAP, lacking the transcriptional activation domain located in the C-terminal, did not affect YAP binding (Supplementary Fig. 2c), it also attenuated YAP-mediated FoxO1 activation (Supplementary Fig. 2d). On the other hand, deletion of the WW domain in YAP (WW) affected neither FoxO1 binding nor YAP-mediated FoxO1 activation (Supplementary Fig. 2c, d). Taken together, these results indicate that both the TEAD binding site and the C-terminal transactivation domain of YAP are important for YAP-mediated FoxO1 activation.

Lats2-YAP axis regulates FoxO1 activity

Phosphorylation of YAP at Ser¹²⁷ by Lats2 promotes nuclear exclusion and cytoplasmic accumulation of YAP, leading to its inactivation¹⁹. In order to examine whether the Hippo signaling pathway regulates FoxO1 through a YAP-dependent mechanism, we overexpressed either Mst1 or Lats2 in cardiomyocytes, since activation of either Mst1 or Lats2 induces a strong Hippo phenotype in the heart^{10,11}, namely promotion of cardiomyocyte apoptosis and suppression of compensatory hypertrophy. Overexpression of Mst1 enhanced the phosphorylation of Ser⁸⁷² and Thr¹⁰⁴¹ of Lats2, indicating full activation of Lats2²⁰, as well as Ser¹²⁷ phosphorylation of YAP (Supplementary Fig. 3a). Lats2 was mainly localized in the nucleus (Supplementary Fig. 3b, c) and overexpression of Lats2 induced nuclear exclusion of YAP (Supplementary Fig. 3d), suggesting that Lats2 activation is sufficient to suppress YAP activity in cardiomyocytes. Luciferase assays revealed that overexpression of Lats2 inhibited, whereas downregulation of Lats2 enhanced, the transcriptional activity of FoxO1 (Fig. 1f). The transcriptional activity of FoxO1 is primarily dependent upon the phosphorylation status of multiple amino acid residues¹⁴. To rule out the possibility that Lats2 regulates FoxO1 activity through direct phosphorylation, an *in vitro* kinase assay was performed, using myc-tagged FoxO1 as a substrate. We observed that FoxO1 was not phosphorylated in the presence of a constitutively active form of Lats2 (Supplementary Fig. 4a). Importantly, downregulation of YAP completely abolished the increase in FoxO1 transcriptional activity observed in the presence of Lats2 knockdown alone (Supplementary Fig. 4b, c). Therefore, these data suggest that the transcriptional activity of FoxO1 is regulated by the Lats2-YAP axis. Since phosphorylation of FoxO1 at Thr²⁴ and Ser²⁵⁶ by Akt induces 14-3-3 binding and cytosolic translocation of FoxO1^{21,22}, we next examined whether transcriptional inactivation of FoxO1 induced by Lats2 activation is mediated by Akt. In cardiomyocytes, overexpression of Lats2 affected neither the activity of Akt, as evaluated by its Ser⁴⁷³ phosphorylation level, nor the level of FoxO1 phosphorylation at Thr²⁴ and Ser²⁵⁶ (Supplementary Fig. 4d). Although overexpression of YAP induced Akt activation, we did not observe significant changes in phosphorylated FoxO1 levels (Supplementary Fig. 4e), indicating that Hippo signaling regulates FoxO1 through Akt-independent mechanisms.

The YAP-FoxO1 complex mediates antioxidant gene expression

In order to examine whether YAP is involved in FoxO1-mediated antioxidant gene expression, chromatin immunoprecipitation (ChIP) was performed using FoxO1 and YAP antibodies in H9C2 myoblast cells. Mapping of the promoter regions of catalase and MnSOD indicated that each promoter has two conserved FoxO1 binding motifs (Fig. 2a), both of which are required for FoxO1 binding and transcriptional activation in response to oxidative stress^{16,17}. After ChIP with YAP antibody, primer sets designed to detect the FoxO1 DNA binding sites in both promoters were used for PCR analysis. These experiments revealed that YAP was present at the FoxO1 binding motifs in the promoter regions of both catalase and MnSOD (Fig. 2b). As expected, ChIP with FoxO1 antibody showed that FoxO1 binds to the same regions. In order to confirm that YAP is co-localized with FoxO1 on the promoters of catalase and MnSOD, sequential ChIPs were conducted. The first ChIP was performed with FoxO1 antibody and the second ChIP was carried out

with either YAP antibody or FoxO1 antibody using the chromatin eluted from the first ChIP. Following the second ChIP, both YAP and FoxO1 were still bound to the FoxO1 binding motifs in the FoxO1-chromatin complex (Fig. 2b), confirming that YAP and FoxO1 are present at the same promoter regions of catalase and MnSOD. In order to examine whether YAP and FoxO1 form a functional complex to regulate antioxidant gene expression, a luciferase vector was generated that contained a minimal promoter region of catalase (catalase-luc), including one FoxO1 DNA-binding site close to the transcriptional start site. Co-transfection of FoxO1 with catalase-luc enhanced the luciferase activity, but this enhancement was completely abolished by YAP knockdown. Co-transfection of YAP with catalase-luc also caused enhanced luciferase activity, which was completely abolished by FoxO1 depletion (Fig. 2c). These results indicate that YAP is an essential co-factor of FoxO1 and is required to maintain its transcriptional activation of antioxidant gene expression.

Hippo signaling suppresses antioxidant gene expression

We next examined the role of the Hippo signaling pathway in the regulation of catalase and MnSOD expression in intact cells, since overexpression of Lats2 is sufficient to suppress FoxO1-mediated transcription (Fig. 1f). ChIP assays revealed that overexpression of Lats2 significantly reduced the amount of YAP present at the FoxO1 binding sites in the promoter regions of catalase and MnSOD (Fig. 3a). Furthermore, the mRNA and protein levels of both catalase and MnSOD were decreased by Lats2 overexpression (Fig. 3b, c). On the other hand, downregulation of Lats2 increased both the mRNA and protein levels of catalase and MnSOD (Fig. 3b, c). The enhancement in catalase-luc activity observed in Lats2 knockdown cells was completely reversed by simultaneous downregulation of either YAP or FoxO1 (Fig. 3d). These data indicate that the Lats2-YAP-FoxO1 nexus is essential for regulating expression of these antioxidant enzymes. Both catalase and MnSOD can effectively convert superoxide and hydrogen peroxide to water in order to prevent ROS accumulation and protect against cell death from oxidative stress. Inhibition of Lats2 reduced myocyte death in response to H₂O₂ treatment, but not when the cells were co-transduced with adenovirus harboring FoxO1 short hairpin RNA (ad-sh-FoxO1) or YAP short hairpin RNA (ad-sh-YAP) (Fig. 3e and Supplementary Fig. 4f), suggesting that Lats2 activation impairs the antioxidant defense and triggers cell death through suppression of YAP-FoxO1. Taken together, these data suggest a novel mechanism in which Hippo signaling activation regulates cell death through suppression of the FoxO1-mediated antioxidant response during oxidative stress.

Hippo activation enhances oxidative stress *in vivo*

We next sought to further assess the physiological implications of our observations. Reperfusion injury occurs when the blood supply resumes after a period of ischemia and causes cell death and dysfunction in critical organs, including the heart and the brain²³. Reperfusion injury is caused primarily by oxidative stress²³. Inactivation of the upstream Hippo pathway kinase, Mst1, has been shown to reduce I/R injury in the heart and attenuate neuron cell death^{10,13}. Immunoblot results revealed that I/R strongly induces phosphorylation of Mst1, Lats2 and YAP (Fig. 4a), suggesting that Hippo signaling is activated during I/R in the heart. Increased phosphorylation of YAP at Ser¹²⁷ and decreased

YAP abundance in the nuclear fraction were observed in wild-type (WT) mice after I/R, effects which were completely attenuated in dominant negative *lats2* (Tg-DN-Lats2) transgenic mice (Fig. 4a, b), in which Lats2 kinase activity is completely suppressed¹¹, suggesting that endogenous Lats2 mediates Ser¹²⁷ phosphorylation and inactivation of YAP in response to I/R. The protein levels of catalase and MnSOD were significantly decreased in WT mice but not in Tg-DN-Lats2, indicating that Hippo activation decreased antioxidant gene expression during I/R *in vivo* (Fig. 4c). The global antioxidant capacity of heart homogenates after I/R was also dramatically decreased in WT mice but not in Tg-DN-Lats2 mice (Fig. 4d). We further investigated the extent of oxidative stress-induced damage during I/R. Tissue samples were stained with anti-8-hydroxydeoxyguanosine (8-OHdG) antibody, a marker of oxidative DNA damage. Immunohistochemistry results revealed that Tg-DN-Lats2 mice exhibited less ROS-induced DNA damage than WT mice after I/R (Supplementary Fig. 5a). In addition, the myocardial GSSG/GSH ratio, an indicator of intracellular redox status, was significantly elevated in WT mice but not in Tg-DN-Lats2 mice (Supplementary Fig. 5b). The size of the myocardial infarct/area-at-risk (AAR), indicative of necrotic cell death, as well as the number of apoptotic TUNEL-positive cells, was significantly smaller in Tg-DN-Lats2 than in WT mice (Supplementary Fig. 6a, b). Furthermore, the same phenotype was observed in mouse models with cardiac-specific deletion of *lats2* (Lats2-CKO) (Supplementary Fig. 7a, b). When we further assessed cardiac I/R injury using *ex vivo* models, we noted a similar decrease in infarct size in Tg-DN-Lats2 mice (Supplementary Fig. 8a), which was accompanied by improved function during the recovery phase of reperfusion, as assessed by left ventricular developed pressure (LVDP) (Supplementary Fig. 8b). In sum, these data provide strong evidence that activation of Hippo signaling mediates oxidative stress-induced injury during I/R.

Inhibition of the YAP-FoxO1 complex mediates I/R injury

If YAP-FoxO1 complex activity is essential for mediating cell survival during I/R, suppression of this complex should abolish the protective effect in Tg-DN-Lats2 mice and reactivation of this complex should rescue WT mice from I/R injury. To test this hypothesis, ad-sh-FoxO1 was injected into the LV and, 5 days later, I/R was performed. The efficacy of adenovirus injection was confirmed by whole-heart β -galactosidase staining in mice injected with Ad-LacZ (Supplementary Fig. 6c). The efficacy of ad-sh-FoxO1 injection was confirmed by immunoblot (Supplementary Fig. 6d). Compared with injection of control short hairpin RNA adenovirus (ad-sh-con), injection of ad-sh-FoxO1 significantly increased infarct size in Tg-DN-Lats2 mice, to the same level as in WT mice (Fig. 5a). Knocking down FoxO1 also significantly increased apoptosis in Tg-DN-Lats2 in response to I/R (Fig. 5b). Since YAP has a direct positive effect on the regulation of the FoxO1-mediated antioxidant response, whether exogenous expression of YAP could rescue myocardial damage induced by I/R was also examined. Adenovirus harboring WT YAP or a constitutively activated YAP mutant (S127A) was injected into the myocardium 3 days before I/R (Supplementary Fig. 6e) and infarct size was examined. Compared to injection of LacZ, both WT and S127A YAP significantly attenuated I/R-induced downregulation of catalase and MnSOD (Fig. 5c) but did not affect e-NOS activity (Supplementary Fig. 6f). Furthermore, injection of adenovirus harboring either WT or S127A YAP decreased the myocardial infarct size and cardiomyocyte apoptosis in response to I/R (Fig. 5d, e),

suggesting that restoration of YAP-FoxO1 prevents cell death in response to oxidative stress induced by I/R.

Discussion

Our results reveal that there is crosstalk between the Hippo-YAP signaling pathway and FoxO1 in regulating cell death in response to oxidative stress (Fig. 6). We discovered that YAP is a novel co-activator of FoxO1, and that the YAP-FoxO1 complex binds to the promoters of catalase and MnSOD, a step which is essential for expression of these antioxidant genes. Activation of the Hippo pathway during I/R inhibits the YAP-FoxO1 complex and suppresses expression of FoxO1 target genes, thereby enhancing oxidative stress and promoting cell death in cardiomyocytes.

FoxO1 activity is regulated by posttranslational modifications (PTMs), including phosphorylation and acetylation¹⁵. Akt phosphorylates FoxO1 at Thr²⁴ and Ser²⁵⁶, thereby inducing nuclear exit of FoxO1. However, overexpression of Lats2 induces nuclear exclusion of YAP without affecting either the activity of Akt or phosphorylation of FoxO1 at Thr²⁴/Ser²⁵⁶ (Supplementary Fig. 3d, 4d). We have shown previously that overexpression of YAP in neonatal cardiomyocytes induces activation of Akt, thereby preventing cardiomyocyte death¹². However, this was not accompanied by phosphorylation of FoxO1 at the Akt sites. These results suggest that YAP-mediated regulation of FoxO1 is independent of Akt-mediated phosphorylation.

Deacetylation of FoxOs by Sirt1 also mediates cell survival during stress conditions²⁴. We have shown previously that Sirt1 deacetylates FoxO1 and facilitates its nuclear translocation, thereby mediating a protective effect against I/R injury in the heart²⁵. We here show that activation of Mst1 and Lats2 in response to I/R induces the nuclear exit of YAP, thereby negatively affecting the transcription of FoxO1 target genes, including catalase and MnSOD, even if FoxO1 is in the nucleus. Thus, although the activity of FoxO1 is regulated through multiple mechanisms, nuclear localization of endogenous YAP appears essential for transcriptional activation of FoxO1 in response to I/R, and this is critically regulated by the Hippo pathway.

Mst1 has been shown to phosphorylate FoxO3, which induces nuclear translocation of FoxO3¹³ but inhibits its high-affinity DNA binding²⁶, suggesting that this upstream component of the Hippo pathway can inhibit FoxOs independently of YAP. Here, however, we show that YAP, one of the terminal effectors of the Hippo pathway, also directly regulates FoxO1. Thus, the activity of FoxOs may be dually regulated by the components of the Hippo pathway; namely, activation of Mst1 and consequent suppression of YAP both negatively regulate transcription through FoxOs. At present, it remains unknown whether the regulation of FoxO by both upstream and downstream components of the Hippo pathway is stimulus-specific or coordinately regulates death and survival of cardiomyocytes.

The transcriptional activity of FoxOs is also regulated by transcriptional cofactors. For example, the interaction between β -catenin and FoxO3 is important to prevent oxidative damage in cancer cell lines and control life span and the aging process in *C. elegans*²⁷. In

hepatocytes, the peroxisome proliferator activated receptor- γ coactivator 1 (PGC-1) interacts with FoxO1 and stimulates target gene expression to control glucose homeostasis²⁸. Here we show that YAP-FoxO1 interaction is essential to mediate antioxidant gene expression in cardiomyocytes. The presence of multiple transcriptional regulators may allow FoxOs to tightly control expression of specific sets of target genes in a coordinated and stimulus-specific manner.

TAZ shares approximately 50% amino acid sequence similarity with. Both YAP and TAZ are negatively regulated by the Hippo pathway, bind to common transcription factors, including the Runx family and TEAD, and play redundant roles in several biological events, including tumorigenesis^{29–31}. In the heart, both YAP and TAZ mediate embryonic heart growth and postnatal myocyte survival^{8,9,12}. The fact that both YAP and TAZ interact with TBX5, a T-box transcription factor, suggests that YAP and TAZ may have overlapping roles during cardiac development³². However, they also have non-overlapping functions. For example, severe cardiac dysfunction results from α MHC-Cre-mediated cardiac-specific deletion of YAP but not of TAZ⁹. On the other hand, genetic deletion of TAZ induces the development of renal cysts³³. Since downregulation of YAP inhibits FoxO1-mediated transcription, we speculate that TAZ may not compensate for the absence of YAP in cardiomyocytes.

One key feature of highly proliferative cells is persistently enhanced ROS generation^{34,35}. To overcome the generally pro-death actions of ROS, cancer cells develop adaptive mechanisms^{36–38} that help the dividing cells escape premature senescence and apoptosis, as well as confer drug resistance to cancer cells³⁵. Forkhead box transcription factors regulate both pro-survival genes and premature senescence^{27,38}, suggesting the potential importance of FoxOs during tumor development and progression. In addition, increasing lines of evidence suggest that the Hippo pathway acts as a tumor suppressor in many organs. Loss-of-function mutations in the Hippo signaling pathway and hyperactivation of YAP have been found in multiple cancers¹. Thus, it is tempting to speculate that regulation of antioxidant genes through the YAP-FoxO1 pathway may be a critical mechanism through which the Hippo pathway regulates tumorigenesis.

In conclusion, our study shows a novel connection between the Hippo pathway and FoxO1 through YAP. Since the Hippo pathway and FoxOs share many important functions, including regulation of growth, death, and survival in cells and regulation of stress resistance and life span in organisms, we speculate that the interaction between YAP and FoxO1 is a point of convergence that allows cells and organisms to precisely control important cellular functions through signals from these two major signaling pathways.

Methods

Transgenic mice

The generation of cardiac-specific dominant negative *lats2* transgenic mice on an FVB background (Tg-DN-Lats2)¹¹, transgenic mice harboring a floxed *Yap1* allele³⁹ on C57BL/6 background, and transgenic mice harboring a floxed *lats2* allele⁴⁰ on C57BL/6 background has been previously described. Cardiac deletion was achieved by crossbreeding with α -

MHC Cre recombinase transgenic mice. Male mice aged 12–16 weeks were used for *in vivo* adenovirus injection and/or ischemia/reperfusion surgery. All animal protocols were approved by the Institutional Animal Care and Use Committee of New Jersey Medical School, Rutgers Biomedical and Health Sciences.

Ischemia/reperfusion surgery *in vivo*

Ischemia/reperfusion was achieved by ligating the anterior descending branch of the left coronary artery (LAD) using an 8–0 prolene suture, with silicon tubing (1 mm OD) placed on top of the LAD, 2 mm below the border between the left atrium and LV. Ischemia was confirmed by ECG change (ST elevation). After occlusion for 45 minutes in mice of an FVB background and for 20–30 minutes in mice of a C57BL/6J background, the silicon tubing was removed to achieve reperfusion and the rib space and overlying muscles were closed. Twenty-four hours after reperfusion, myocardial infarction was examined. To demarcate the ischemic area at risk (AAR), Alcian blue dye (1%) was perfused into the aorta and coronary arteries. Hearts were excised and LVs were sliced into 1-mm-thick cross-sections. The heart sections were then incubated with a 1% triphenyltetrazolium chloride solution at 37°C for 15 minutes. The infarct area (pale), the AAR (not blue), and the total LV area from both sides of each section were measured using Adobe Photoshop (Adobe Systems Inc.), and the values obtained were averaged. The percentage of area of infarction and AAR of each section were multiplied by the weight of the section and then totaled from all sections. AAR/LV and infarct area/AAR were expressed as percentages²⁵.

Langendorff-perfused mouse heart model of global I/R

Mouse hearts were mounted on a Langendorff-type isolated heart perfusion system and subjected to retrograde coronary artery reperfusion with 37°C oxygenated Krebs-Henseleit bicarbonate buffer (120 mM NaCl, 17 mM Glucose, 25 mM NaHCO₃, 5.9 mM KCl, 1.2 mM MgCl₂, 2.5 mM CaCl₂, 0.5 mM EDTA), pH 7.4, at a constant pressure of 80 mmHg. A balloon filled with water was introduced into the left ventricle (LV) through the mitral valve orifice and connected to a pressure transducer via a plastic tube primed with water. LV pressures and LV dP/dt were recorded with a strip chart recorder (Astro-Med, Inc). The LV end-diastolic pressure was set at 4–10 mmHg at the beginning of perfusion by adjusting the volume of the balloon in the LV and the volume was kept constant throughout the experiment. After a 30 minute equilibration period, the heart was subjected to 30 minutes of global ischemia (at 37°C) followed by 60 minutes of reperfusion²⁵.

Cell cultures

H9C2 myoblast cells and Cos7 cells (American Type Culture Collection) were cultured at 37°C in DMEM/F-12 (Life Technologies, Inc.) with 10% FBS. Primary cultures of ventricular cardiomyocytes were prepared from 1-day-old Crl: (WI) BR-Wistar rats (Harlan Laboratories). A cardiomyocyte-rich fraction was obtained by centrifugation through a discontinuous Percoll gradient. Cells were cultured in complete medium containing DMEM/F-12 supplemented with 5% horse serum, 4 µg/ml transferrin, 0.7 ng/ml sodium selenite (Life Technologies, Inc.), 2 g/l bovine serum albumin (fraction V), 3 mM pyruvic acid, 15 mM HEPES, 100 µM ascorbic acid, 100 µg/ml ampicillin, 5 µg/ml linoleic acid, and 100 µM

5-bromo-2'-deoxyuridine (Sigma). Myocytes were changed to serum-free medium 24 hours before any experiment.

Plasmids

The mammalian expression vector for YAP (pHA-YAP) was generated by insertion of YAP cDNA into pcDNA3-HA, which contains a DNA fragment encoding the HA (GGATCTACCCATACGATGTTCCGGATTACGCTAGTCTCTAGTCGAC; YPYDVPDYASL) tag inserted downstream of the CMV promoter of pcDNA3. Site-directed mutagenesis was performed to generate pHA-YAP (S94A) using the QuikChange mutagenesis kit (Agilent Technologies). The expression vector for YAP with deleted WW domain (pHA-YAP WW) was generated by PCR. The expression vector for YAP with N-terminal fragment (pHA-YAP N-terminal) was generated by insertion of YAP cDNA from amino acid 1-316 into pcDNA3-HA.

Adenovirus constructs

Adenovirus harboring Lats2 and Mst1 has been described¹¹. Adenoviruses harboring sh-RNA for Lats2 (Ad-sh-Lats2), FoxO1 (Ad-sh-FoxO1) and YAP (Ad-sh-YAP) were generated as previously described using the following hairpin-forming oligos. For Lats2: 5'-GCAGGTTCTTCGACGACAATTCAAGAGATTGTCGTCGAAGAACCTGCCTTT TTT-3'; For FoxO1: 5'-CGCCAAACTCACTACACCATTTC AAGAGAATGGTGTAGTGAGTTTGGCTTTTTT-3'; For YAP: 5'-GGTCAGAGATACTTCTTAATTCAAGAGATTAAGAAGTATCTCTGACCTTTTTT-3'. The hairpin loop sequence is underlined. The adenoviruses used for *in vivo* injection were purified using the Adeno-X™ Maxi Purification Kit (Clontech).

Antibodies

Antibodies used for immunoblots were purchased from the indicated companies: Catalase (1:3000 dilution, #ab1877) (Abcam), p-Akt (Ser473) (1:2000 dilution, #9272), Akt (1:2000 dilution, #9271), p-eNOS (Ser1177) (1:1000 dilution, #9571), eNOS (1:1000 dilution, #9586), p-FoxO1 (Thr24, Ser256) (1:1000 dilution, #9464 and #9461), FoxO3 (1:1000 dilution, #9467), GAPDH (1:3000 dilution, #2118), Histone H3 (1:500 dilution, #9715), Lamin A/C (1:5000 dilution, #4777), p-Mst1 (Thr183) (1:1000 dilution, #3681), p-YAP (Ser127) (1:1000 dilution, #4911), YAP (1:2000 dilution, #4912) (Cell Signaling Technology), FoxO1 (1:2000 dilution, #1874-1) (epitomics), α -tubulin (1:5000 dilution, #T-6199), FLAG (1:2000 dilution, #F3165) (Sigma), MnSOD (1:3000 dilution, #611580), Mst1 (1:2000 dilution, #611052) (BD Biosciences), and Lats2 (1:1000 dilution, #ab54073 and #A300-479A) (Abcam and Bethyl Laboratories). The p-Lats2 (S872 and T1041) (1:500 dilution) antibodies were generated as described⁴¹.

Immunoblot analysis

Heart homogenates or cell lysates were prepared using RIPA buffer containing 50 mM Tris (pH 7.4), 150 mM NaCl, 1% Triton X-100, 0.1% SDS, 1% deoxycholic acid, 1 mM EDTA, 1 mM Na₃VO₄, 1 mM NaF, 0.5 mM 4-(2-aminoethyl) benzenesulfonyl fluoride

hydrochloride, 0.5 µg/ml aprotinin, and 0.5 µg/ml leupeptin. Equal amounts of protein (10–20 µg) were subjected to 10–15% SDS-PAGE. The nuclear and cytosolic fractions were prepared with NE-PER Nuclear and Cytoplasmic Extraction Reagents (Pierce). After proteins were transferred to a PVDF membrane, immunoblots were probed with the indicated antibodies. Full scans of all western blots and gels are supplied in Supplementary Figure 9.

Immunoprecipitation

Heart homogenates or cell lysates were prepared using a lysis buffer containing 50 mM Tris (pH 7.4), 150 mM NaCl, 1% Triton X-100, and 1 mM EDTA. The lysates were incubated with protein A agarose-immobilized antibody for 2 hours at 4°C. After immunoprecipitation, the immunocomplexes were washed with lysis buffer three times and eluted with 2x SDS sample buffer.

Immunocytochemistry

Neonatal cardiomyocytes in 4-well chambers were washed with phosphate-buffered saline (PBS) three times, fixed with 4% paraformaldehyde for 15 minutes, permeabilized in 0.3% Triton X-100 for 10 minutes, and blocked with 3% bovine serum albumin for 1 hour at room temperature. The following primary antibodies were used: Lats2 (1:200 dilution, #ab54073) (Abcam), FoxO1 (1:100 dilution, #1874-1) (epitomics), YAP (1:100 dilution, H00010413-M01) (Abnova), and α -actinin (1:400 dilution, A7811) (Sigma). Alexa Fluor 488 Dye- or Alexa Fluor 594 Dye-conjugated secondary antibody (Invitrogen) was used for detecting indirect fluorescence. Slides were mounted using a reagent containing DAPI (VECTASHIELD; Vector Laboratories Inc.).

In situ PLA

Neonatal cardiomyocytes were fixed, permeabilized, and blocked as described as above. Heart sections were deparaffinized with xylene, rehydrated in graded alcohol concentrations, briefly washed in water, and then antigen-unmasked using citrate buffer and blocked in 5% goat serum in PBST for 1 hour. *In situ* PLA experiments were performed as described previously^{42,43}. Incubation with primary antibodies (Rabbit FoxO1 and Mouse YAP in blocking solution) was performed at room temperature for 2 hours. Cells or heart sections were washed 3× for 5 minutes in PBS plus 0.1% Tween 20. The protein–protein interaction between FoxO1 and YAP was detected with secondary proximity probes (Rabbit-PLUS and Mouse-MINUS, Olink Biosciences AB). The secondary proximity probes were incubated for 1 hour at 37°C. Cells were washed 1× for 5 minutes in 10 mM Tris-HCl (pH 7.5) plus 0.1% Tween 20 at 37°C, then 2× for 5 minutes in PBS plus 0.1% Tween 20. All subsequent steps were performed according to the Duolink proximity ligation assay detection kit protocol (Olink Biosciences AB).

Immunohistochemistry for 8-OHdG staining

Anti-8-hydroxy-2'-deoxyguanosine (anti-8-OHdG) antibody (Oxis International Inc.) was diluted to 7.5 µg/ml in PBS and applied to tissue sections for 2 hours at room temperature. The immunohistochemistry experiment was performed using the ImmunoCruz staining

system (streptavidin-biotin peroxidase method, Santa Cruz Biotechnology), and sections were counterstained with hematoxylin.

X-Gal Staining

Heart tissues were fixed for 1 hour in 0.1 M phosphate buffer (pH 7.3) supplemented with 5 mM EGTA, 2 mM MgCl₂, and 0.2% glutareldahyde (Sigma). Fixed samples were washed 3× for 15 minutes with 0.1 M phosphate buffer (pH 7.3) supplemented with 2 mM MgCl₂, 0.01% Na deoxycholate, and 0.02% NP-40 and then incubated in staining buffer containing 0.1 M phosphate buffer (pH 7.3), 2 mM MgCl₂, 5 mM potassium ferrocyanide, 5 mM potassium ferricyanide, 0.01% Na deoxycholate, 0.02% NP-40 and X-gal at a final concentration of 1 mg/ml overnight at 37°C.

Detection of oxidative stress

Fresh heart tissues were dissected and incubated in a Krebs/HEPES buffer containing 5μM lucigenin. After 15 minutes of equilibration, counts were obtained every minute for the next 5 minutes in a luminometer. The O₂⁻ level was presented as chemiluminescence units normalized by tissue weight. For H₂O₂ production, heart sections were incubated with Amplex Red (10 μM) for 30 minutes at 37°C. The Amplex assay was performed according to the supplier's protocol (Molecular Probes).

Tissue homogenates were prepared using 5% Metaphosphoric Acid. The tissue level of oxidized glutathione/reduced glutathione (GSSG/GSH) was determined using the Bioxytech GSH/GSSG-412 kit (Oxis International Inc.). The antioxidant capacity of heart homogenates was determined using an antioxidant assay kit according to the supplier's instructions (Cayman Chemical).

RT-PCR and quantitative PCR

Total RNA was isolated from neonatal cardiomyocytes using TRIzol (Invitrogen) and first-strand cDNA was synthesized using the ThermoScript RT-PCR system (Invitrogen). Quantitative PCR was carried out using a DNA Engine Opticon 2 system (Bio-Rad) and iQ SYBR Green Supermix (Bio-Rad). Catalase and MnSOD mRNA levels were analyzed using specific primers. Values were standardized using β-actin. q-PCR primers: catalase: forward: CCTCCTCGTTCAAGATGTGGTTT, reverse: CCTT TGCCTTGGAGTATCTGGTAATA; MnSOD: forward: CAACTCAGGTTGCTCTTCA, reverse: CGACCTTGCTCCTTATTGA; β-actin forward: AGGCCAACCGTGAAAAGA TG, reverse: ACCAGAGGCATACAGGGACAA.

CellTiter-Blue assay

Cell viability was measured by CellTiter-Blue (CTB) assays (Promega). In brief, cardiomyocytes (1 × 10⁵ per 100 μl) were seeded onto 96-well dishes. After 24 hours, the cells were transduced with the indicated adenovirus. After transduction, myocytes were incubated with or without H₂O₂ treatment. Viable cell numbers were measured by the CTB assay. The CTB assays were performed according to the supplier's protocol.

Transient transfection and luciferase assays

Cells were plated on 12-well plates and transfected with 1 μ g of the indicated luciferase vectors using Fugene 6. Total DNA quantity was kept constant. Six hours after transfection, the cells were washed and transduced with the indicated adenovirus. The cells were lysed with Passive Lysis Buffer, and the transcriptional activity was determined using a luciferase assay system (Promega).

In vitro kinase assay

Ten ng of active Lats2 recombinant protein (Signal Chem) was incubated with 1 μ g myc-FoxO1 recombinant protein (OriGene) in a kinase assay buffer containing 25 mM MOPS (pH 7.2), 12.5 mM β -glycerolphosphate, 25 mM $MgCl_2$, 5 mM EGTA, 2 mM EDTA, and 0.25 mM DTT. The reaction was initiated by adding [γ - ^{32}P] ATP (Perkin Elmer) and was incubated for 30 minutes at 30°C. The reaction was terminated by the addition of 2x SDS sample buffer. Samples were separated by SDS-PAGE and the dried gel was subjected to autoradiography.

Chromatin immunoprecipitation (ChIP) and sequential ChIP

H9C2 myoblasts were treated with 1% formaldehyde for 10 minutes to cross-link proteins and chromatin. The reaction was stopped by adding 0.125 M Glycine for 5 minutes. Cells were washed with cold PBS twice. Cells were then resuspended in 1 ml ChIP lysis buffer (20 mM Tris-HCl (pH 8.0), 85 mM KCl, 0.5% NP-40) for 10 minutes at 4°C and centrifuged at 5,000 rpm to pellet the nuclei. The cell nuclei were resuspended in 400 μ L nuclei lysis buffer (50 mM Tris-HCl (pH 8.0), 10 mM EDTA, 1% SDS) and then subjected to sonication 5 times for 30 seconds with 30 second intervals. Purified chromatin was analyzed on a 1% agarose gel to determine the shearing efficiency. As a control, normal IgG was used as a replacement for YAP or FoxO1 antibody (Santa Cruz Biotechnology). For sequential ChIP, sheared chromatin was first immunoprecipitated with FoxO1, followed by elution and a second immunoprecipitation using the YAP antibody. The ChIP procedure was performed as in the supplier's protocol (Active Motif). ChIP-PCR primers: Catalase promoter-DBE1: forward: GGTGGACTATTGACAGTGT TGGG, reverse: CGCCATCCAGTTATTTACTCAGG; Catalase promoter-DBE2: forward: ACCAAATAAATAAGCAAAGTGAG, reverse: GAAACTCTAGAAGGGAC AGGATT; MnSOD promoter-DBE1: Forward: TCATGGCCACTATGCCTCAA, reverse: TCTCAGCTGTGTCTCTTCC; MnSOD promoter-DBE2: forward: CCTCTTG TTTATTACATCAAGATTG, reverse: CTGGTTGTCAACTTGACTATATC.

Statistical Analysis

All values are expressed as mean \pm s.e.m.. Statistical analysis between groups was conducted by unpaired Student's t-test or one-way ANOVA followed by a Newman-Keuls comparison test. Values of $p < 0.05$ were considered to be significant.

Supplementary Material

Refer to Web version on PubMed Central for supplementary material.

Acknowledgments

We thank Daniela Zablocki and Christopher D. Brady for critical reading of the manuscript. This work was supported in part by U.S. Public Health Service Grants HL67724, HL91469, HL102738, HL112330, and AG23039 (JS), the Foundation of Leducq Transatlantic Network of Excellence (JS), and the National Creative Research Program (2010-001827) (DSL).

References

1. Pan D. The hippo signaling pathway in development and cancer. *Dev Cell*. 2010; 19:491–505. [PubMed: 20951342]
2. Zhou D, et al. Mst1 and Mst2 maintain hepatocyte quiescence and suppress hepatocellular carcinoma development through inactivation of the Yap1 oncogene. *Cancer Cell*. 2009; 16:425–438. [PubMed: 19878874]
3. Zhou D, et al. Mst1 and Mst2 protein kinases restrain intestinal stem cell proliferation and colonic tumorigenesis by inhibition of Yes-associated protein (Yap) overabundance. *Proc Natl Acad Sci U S A*. 2011; 108:E1312–1320. [PubMed: 22042863]
4. Dong JX, et al. Elucidation of a universal size-control mechanism in *Drosophila* and mammals. *Cell*. 2007; 130:1120–1133. [PubMed: 17889654]
5. Voorhoeve PM, et al. A genetic screen implicates miRNA-372 and miRNA-373 as oncogenes in testicular germ cell tumors. *Cell*. 2007; 131:102–114.
6. Tapon N, et al. salvador promotes both cell cycle exit and apoptosis in *Drosophila* and is mutated in human cancer cell lines. *Cell*. 2002; 110:467–478. [PubMed: 12202036]
7. Heallen T, et al. Hippo Pathway Inhibits Wnt Signaling to Restrain Cardiomyocyte Proliferation and Heart Size. *Science*. 2011; 332:458–461. [PubMed: 21512031]
8. Xin M, et al. Regulation of Insulin-Like Growth Factor Signaling by Yap Governs Cardiomyocyte Proliferation and Embryonic Heart Size. *Sci Signal*. 2011; 4 ARTN ra70. 10.1126/scisignal.2002278
9. Xin M, et al. Hippo pathway effector Yap promotes cardiac regeneration. *Proc Natl Acad Sci U S A*. 2013.1073/pnas.1313192110
10. Yamamoto S, et al. Activation of Mst1 causes dilated cardiomyopathy by stimulating apoptosis without compensatory ventricular myocyte hypertrophy. *J Clin Invest*. 2003; 111:1463–1474. [PubMed: 12750396]
11. Matsui Y, et al. Lats2 is a negative regulator of myocyte size in the heart. *Circ Res*. 2008; 103:1309–1318. [PubMed: 18927464]
12. Del Re DP, et al. Yes-associated Protein Isoform 1 (Yap1) Promotes Cardiomyocyte Survival and Growth to Protect against Myocardial Ischemic Injury. *J Biol Chem*. 2013; 288:3977–3988. [PubMed: 23275380]
13. Lehtinen MK, et al. A conserved MST-FOXO signaling pathway mediates oxidative-stress responses and extends life span. *Cell*. 2006; 125:987–1001. [PubMed: 16751106]
14. Calnan DR, Brunet A. The FoxO code. *Oncogene*. 2008; 27:2276–2288. [PubMed: 18391970]
15. Huang H, Tindall DJ. Dynamic FoxO transcription factors. *J Cell Sci*. 2007; 120:2479–2487. [PubMed: 17646672]
16. Nemoto S, Finkel T. Redox regulation of forkhead proteins through a p66shc-dependent signaling pathway. *Science*. 2002; 295:2450–2452. [PubMed: 11884717]
17. Kops GJ, et al. Forkhead transcription factor FOXO3a protects quiescent cells from oxidative stress. *Nature*. 2002; 419:316–321. [PubMed: 12239572]
18. Sengupta A, Molkenin JD, Paik JH, DePinho RA, Yutzey KE. FoxO Transcription Factors Promote Cardiomyocyte Survival upon Induction of Oxidative Stress. *J Biol Chem*. 2011; 286:7468–7478. [PubMed: 21159781]
19. Zhao B, et al. Inactivation of YAP oncoprotein by the Hippo pathway is involved in cell contact inhibition and tissue growth control. *Gene Dev*. 2007; 21:2747–2761. [PubMed: 17974916]
20. Chan EH, et al. The Ste20-like kinase Mst2 activates the human large tumor suppressor kinase Lats1. *Oncogene*. 2005; 24:2076–2086. [PubMed: 15688006]

21. Tang ED, Nunez G, Barr FG, Guan KL. Negative regulation of the forkhead transcription factor FKHR by Akt. *J Biol Chem.* 1999; 274:16741–16746. [PubMed: 10358014]
22. Brunet A, et al. 14-3-3 transits to the nucleus and participates in dynamic nucleocytoplasmic transport. *J Cell Biol.* 2002; 156:817–828. [PubMed: 11864996]
23. Murphy E, Steenbergen C. Mechanisms underlying acute protection from cardiac ischemia-reperfusion injury. *Physiol Rev.* 2008; 88:581–609. [PubMed: 18391174]
24. Brunet A, et al. Stress-dependent regulation of FOXO transcription factors by the SIRT1 deacetylase. *Science.* 2004; 303:2011–2015. [PubMed: 14976264]
25. Hsu CP, et al. Silent information regulator 1 protects the heart from ischemia/reperfusion. *Circulation.* 2010; 122:2170–2182. [PubMed: 21060073]
26. Brent MM, Anand R, Marmorstein R. Structural basis for DNA recognition by FoxO1 and its regulation by posttranslational modification. *Structure.* 2008; 16:1407–1416. [PubMed: 18786403]
27. Essers MA, et al. Functional interaction between beta-catenin and FOXO in oxidative stress signaling. *Science.* 2005; 308:1181–1184. [PubMed: 15905404]
28. Puigserver P, et al. Insulin-regulated hepatic gluconeogenesis through FOXO1-PGC-1alpha interaction. *Nature.* 2003; 423:550–555. [PubMed: 12754525]
29. Zhang H, et al. TEAD transcription factors mediate the function of TAZ in cell growth and epithelial-mesenchymal transition. *J Biol Chem.* 2009; 284:13355–13362. [PubMed: 19324877]
30. Zhao B, Lei QY, Guan KL. The Hippo-YAP pathway: new connections between regulation of organ size and cancer. *Curr Opin Cell Biol.* 2008; 20:638–646. [PubMed: 18955139]
31. Kanai F, et al. TAZ: a novel transcriptional co-activator regulated by interactions with 14-3-3 and PDZ domain proteins. *The EMBO journal.* 2000; 19:6778–6791. [PubMed: 11118213]
32. Murakami M, Nakagawa M, Olson EN, Nakagawa O. A WW domain protein TAZ is a critical coactivator for TBX5, a transcription factor implicated in Holt-Oram syndrome. *Proc Natl Acad Sci U S A.* 2005; 102:18034–18039. [PubMed: 16332960]
33. Hossain Z, et al. Glomerulocystic kidney disease in mice with a targeted inactivation of Wwtr1. *Proc Natl Acad Sci U S A.* 2007; 104:1631–1636. [PubMed: 17251353]
34. Cairns RA, Harris IS, Mak TW. Regulation of cancer cell metabolism. *Nat Rev Cancer.* 2011; 11:85–95. [PubMed: 21258394]
35. Trachootham D, Alexandre J, Huang P. Targeting cancer cells by ROS-mediated mechanisms: a radical therapeutic approach? *Nat Rev Drug Discov.* 2009; 8:579–591. [PubMed: 19478820]
36. Sablina AA, et al. The antioxidant function of the p53 tumor suppressor. *Nat Med.* 2005; 11:1306–1313. [PubMed: 16286925]
37. Hu YM, et al. Mitochondrial manganese-superoxide dismutase expression in ovarian cancer. *J Biol Chem.* 2005; 280:39485–39492. [PubMed: 16179351]
38. Park HJ, et al. FoxM1, a critical regulator of oxidative stress during oncogenesis. *The EMBO journal.* 2009; 28:2908–2918. [PubMed: 19696738]
39. Zhang NL, et al. The Merlin/NF2 Tumor Suppressor Functions through the YAP Oncoprotein to Regulate Tissue Homeostasis in Mammals. *Dev Cell.* 2010; 19:27–38. [PubMed: 20643348]
40. Kim M, et al. cAMP/PKA signalling reinforces the LATS-YAP pathway to fully suppress YAP in response to actin cytoskeletal changes. *The EMBO journal.* 2013; 32:1543–1555. [PubMed: 23644383]
41. Yabuta N, et al. Lats2 is an essential mitotic regulator required for the coordination of cell division. *J Biol Chem.* 2007; 282:19259–19271. [PubMed: 17478426]
42. Mahmoudi S, et al. WRAP53 Is Essential for Cajal Body Formation and for Targeting the Survival of Motor Neuron Complex to Cajal Bodies. *Plos Biol.* 2010; 8 Artn E1000521. 10.1371/Journal.Pbio.1000521
43. Jarvius M, et al. In situ detection of phosphorylated platelet-derived growth factor receptor beta using a generalized proximity ligation method. *Molecular & Cellular Proteomics.* 2007; 6:1500–1509. [PubMed: 17565975]

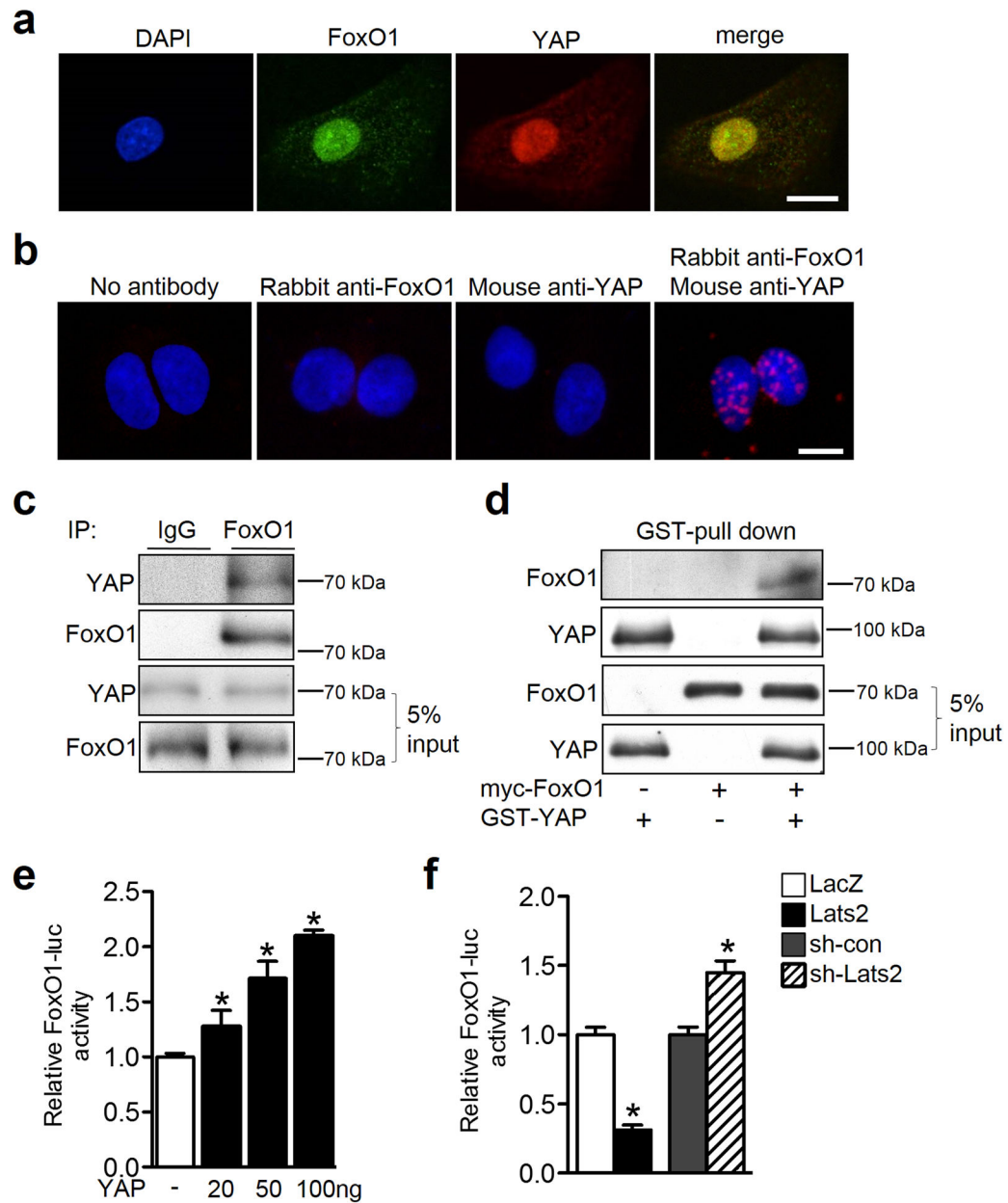


Figure 1. YAP interacts with FoxO1 and regulates its transcriptional activity

a, The localization of FoxO1 and YAP was examined. Myocytes were stained with FoxO1 (red), YAP (green) and DAPI (blue). Scale bar, 10 μ m. **b**, Cells were stained with Rabbit anti-FoxO1 antibody and/or Mouse anti-YAP antibody, and *in vivo* protein-protein interaction between FoxO1 and YAP (red dots) was detected with secondary proximity probes, anti-Rabbit PLUS and anti-Mouse MINUS, using the Duolink *in situ* PLA detection kit. Scale bar, 10 μ m. **c**, Neonatal cardiomyocyte lysates were prepared and immunoprecipitated with FoxO1 antibody or control IgG. The interaction between FoxO1 and YAP was examined. Immunoblots of input lysate controls (5% of inputs) are also shown. **d**, Recombinant GST-YAP and myc-FoxO1 were used to examine the direct

interaction between YAP and FoxO1. **e**, Cardiomyocytes were co-transfected with 1 μ g FoxO1-luc vector and the indicated expression vectors. After 48 hours, the luciferase activity was measured, demonstrating that YAP enhanced FoxO1 transcriptional activity (* $p < 0.05$ vs. empty vector, $n = 3$). **f**, Overexpression of Lats2 inhibited, whereas knockdown of Lats2 enhanced, FoxO1 activity. Cardiomyocytes were transfected with 1 μ g FoxO1-luc vector. After 6 hours, myocytes were transduced with the indicated virus and luciferase activity was measured (* $p < 0.05$ vs. LacZ or sh-con, $n = 3$). Data shown as mean \pm s.e.m.. *P* values were determined using unpaired Student's *t*-test.

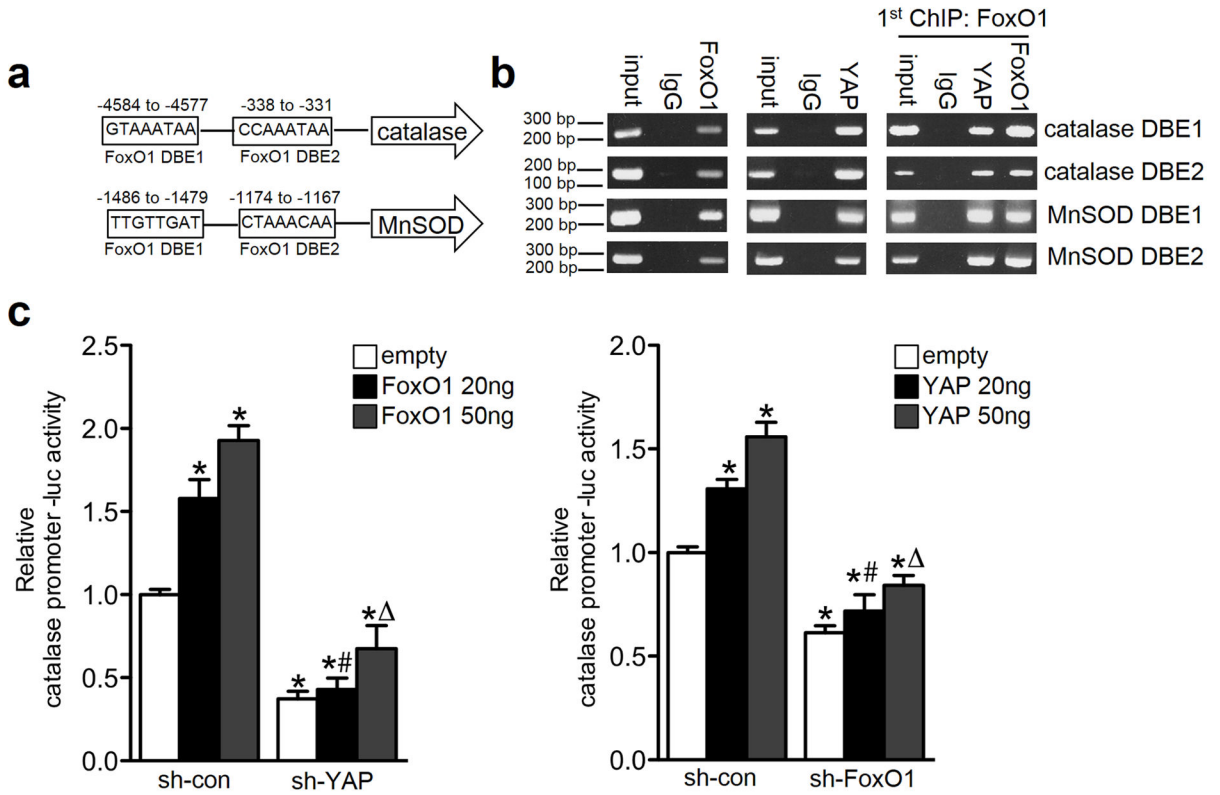


Figure 2. YAP is essential for FoxO1-mediated antioxidant gene expression

a, The catalase and MnSOD promoters contain two potential FoxO1 DNA-binding elements, referred to as DBE1 and DBE2. **b**, ChIP analysis of *in vivo* YAP and FoxO1 binding to the catalase and MnSOD promoters. Protein-bound chromatin was prepared from H9C2 myoblasts and immunoprecipitated with YAP or FoxO1 antibodies. For sequential ChIP, the protein-bound chromatin was first immunoprecipitated with the FoxO1 antibody. The second ChIP was then performed on the chromatin eluted from the first ChIP by immunoprecipitating it with the YAP antibody. Normal IgG was used as a negative control. The immunoprecipitated DNA was analyzed by PCR using primers flanking each of the DBEs. Results are representative of three individual experiments. **c**, The minimal catalase promoter containing FoxO1 DBE2 was cloned into a luciferase vector. Cardiomyocytes were co-transfected with the catalase-luc vector and the indicated expression vectors. After 6 hours, myocytes were transduced with the indicated virus and, after 72 hours, the luciferase activity was measured (* $p < 0.05$ vs. empty vector, # $p < 0.05$ vs. 20ng FoxO1 or YAP, $p < 0.05$ vs. 50ng FoxO1 or YAP, $n = 3$). Data shown as mean \pm s.e.m.. *P* values were determined using one-way ANOVA followed by a Newman-Keuls comparison test.

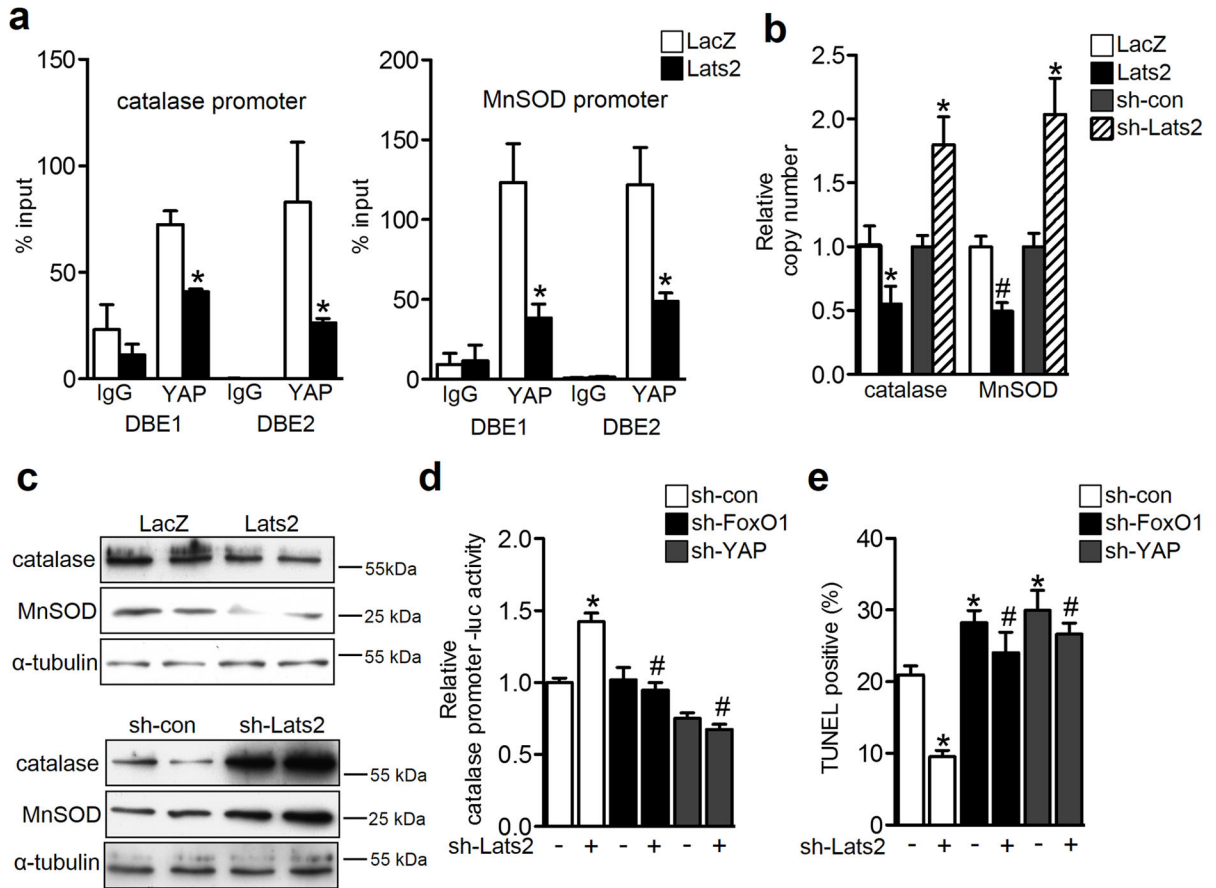


Figure 3. Hippo activation promotes cell death in response to oxidative stress

a, ChIP analysis of *in vivo* YAP binding to the catalase and MnSOD promoters. H9C2 myoblasts were transduced with the indicated adenovirus for 48 hours. Protein-bound chromatin was prepared and immunoprecipitated with IgG and YAP antibodies. The relative occupancy on the promoters was compared with the input signal (**p*<0.05 vs. LacZ, *n*=3).

b–c, Overexpression of Lats2 reduced, whereas knockdown of Lats2 enhanced, catalase and MnSOD protein and mRNA levels. Cardiomyocytes were transduced with the indicated adenovirus. **b**, The mRNA levels of catalase and MnSOD were examined by quantitative RT-PCR. The relative copy number was normalized with β -actin (**p*<0.05 vs. LacZ or sh-con, #*p*<0.01 vs. LacZ, *n*=4).

c, Lysates were used for immunoblot analysis of catalase, MnSOD and α -tubulin. Results are representative of three individual experiments.

d, Cardiomyocytes were transfected with the catalase-luc vector. After 6 hours, myocytes were transduced with the indicated virus and, after 72 hours, luciferase activity was measured (**p*<0.05 vs. sh-con/sh-Lats2(-), #*p*<0.05 vs. sh-con/sh-Lats2(+), *n*=3).

e, Downregulation of Lats2 prevented H₂O₂-induced cell death. Cardiomyocytes transduced with the indicated adenovirus were treated with 100 μ M H₂O₂, and TUNEL-positive cells were examined (**p*<0.05 vs. sh-con/sh-Lats2(-), #*p*<0.05 vs. sh-con/sh-Lats2(+), *n*=4). Data shown as mean \pm s.e.m.. *P* values were determined using unpaired Student's *t*-test or one-way ANOVA followed by a Newman-Keuls comparison test.

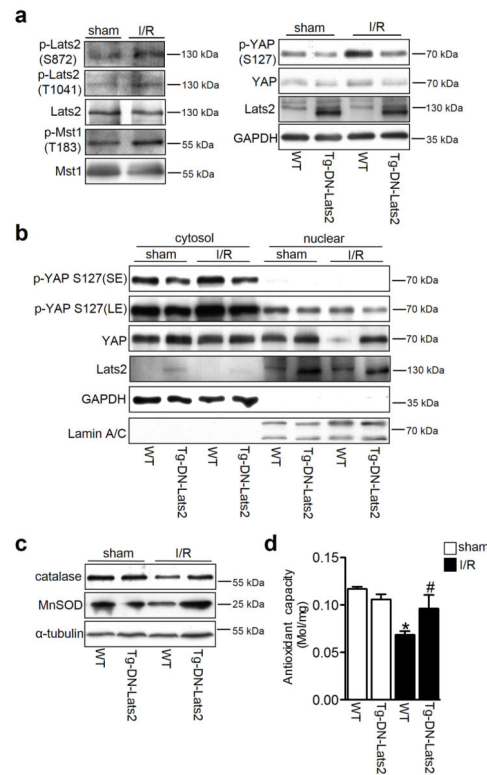


Figure 4. Hippo activation stimulates oxidative stress in response to I/R

a, Representative immunoblots indicating that I/R activated Hippo signaling. Left, WT mice were subjected to ischemia for 45 minutes followed by 2 hours of reperfusion. Sham and ischemic area samples were used for immunoblot analysis for p-Lats2 (T1041 and S872), Lats2, p-Mst1 (Thr183), and Mst1. Right, Tg-DN-Lats2 and control WT mice were subjected to ischemia for 45 minutes followed by 2 hours of reperfusion. Sham and ischemic area samples were used for immunoblot analysis for p-YAP (S127), YAP, Lats2, and GAPDH. The enhancement in YAP phosphorylation during I/R was attenuated in Tg-DN-Lats2, confirming that Lats2 activation was suppressed. **b**, Tg-DN-Lats2 and control WT mice were subjected to ischemia for 45 minutes followed by 2 hours of reperfusion. The cytosolic and nuclear fractions of heart homogenates were prepared and subjected to immunoblot analysis of p-YAP (S127), YAP, Lats2, GAPDH, and Lamin A/C (SE, short exposure; LE, long exposure). **c–d**, Activation of Lats2 decreased antioxidant protein levels and enhanced oxidative stress during I/R. Tg-DN-Lats2 and control WT mice were subjected to ischemia for 45 minutes followed by 24 hours of reperfusion. **c**, Sham and ischemic area samples were used for immunoblot analysis for catalase, MnSOD, and α -tubulin. **d**, The antioxidant capacity of the myocardium was examined (* $p < 0.05$ vs. WT/sham, # $p < 0.05$ vs. WT/I/R, $n = 4$). Data shown as mean \pm s.e.m.. P values were determined using one-way ANOVA followed by a Newman-Keuls comparison test.

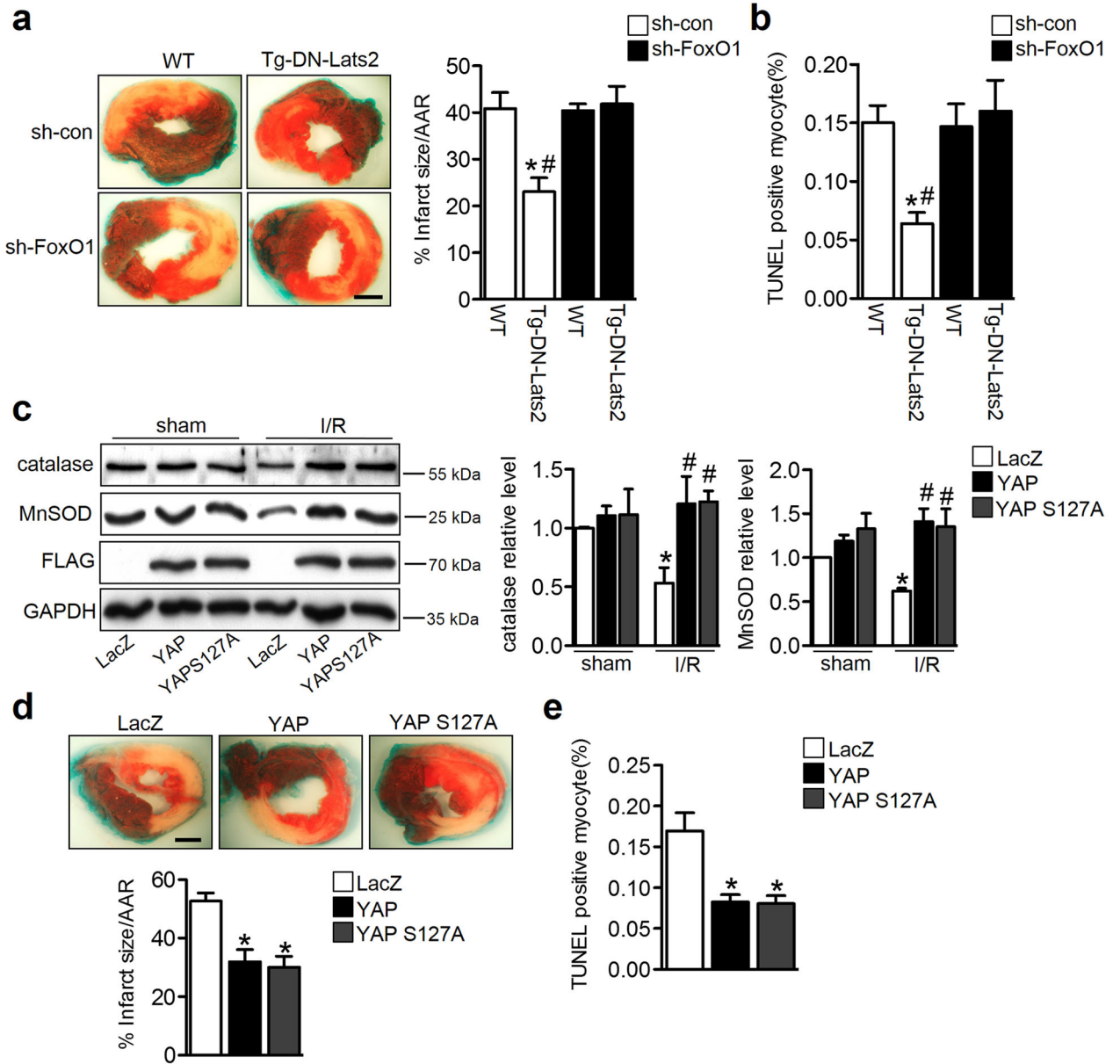


Figure 5. Inhibition of Hippo protects against I/R injury

a–b, Purified adenovirus (1×10^9 opu) was administered by direct injection to the LV free wall (two sites, 25 μ l/site) of Tg-DN-Lats2 and WT mice. I/R surgery was performed 5 days after injection. Mice were subjected to ischemia for 45 minutes followed by 24 hours of reperfusion. **a**, Gross appearance of LV tissue sections after Alcian blue and triphenyltetrazolium chloride staining demonstrates that injection of ad-sh-FoxO1 abolished the protection observed in Tg-DN-Lats2 mice. Quantitative measurement of myocardial infarct area/area at risk (% infarct size/AAR) was performed (* $p < 0.05$ vs. WT/sh-con, # $p < 0.05$ vs. Tg-DN-Lats2/sh-FoxO1, $n = 8$). Scale bar, 1 mm. **b**, LV myocardial sections were subjected to TUNEL staining. The number of TUNEL-positive myocytes was expressed as a percentage of total nuclei detected by DAPI staining (* $p < 0.05$ vs. WT/sh-

con, #p<0.05 vs. Tg-DN-Lats2/sh-FoxO1, n=5–8). **c–e**, Purified adenovirus (1×10^9 opu) was administered by direct injection to the LV free wall (two sites, 25 μ l/site). I/R surgery was performed 3 days after injection. Mice were subjected to ischemia for 30 minutes followed by 24 hours of reperfusion. **c**, Sham and ischemic area samples were used for immunoblot analysis for catalase, MnSOD, and GAPDH. FLAG was also used to examine exogenous YAP gene expression. Statistical analyses of densitometric measurements of catalase and MnSOD are shown (*p<0.05 vs. LacZ/sham, #p<0.05 vs. LacZ/I/R, n=5). **d**, Gross appearance of LV tissue sections after Alcian blue and triphenyltetrazolium chloride staining demonstrates that injection of YAP or YAP S127A decreased the infarct area. Quantitative measurement of myocardial infarct area/area at risk (% infarct size/AAR) was performed (*p<0.05 vs. LacZ, n=8). Scale bar, 1 mm. **e**, LV myocardial sections were subjected to TUNEL staining. The number of TUNEL-positive myocytes was expressed as a percentage of total nuclei detected by DAPI staining (*p<0.05 vs. LacZ, n=5–6). Data shown as mean \pm s.e.m.. *P* values were determined using one-way ANOVA followed by a Newman-Keuls comparison test.

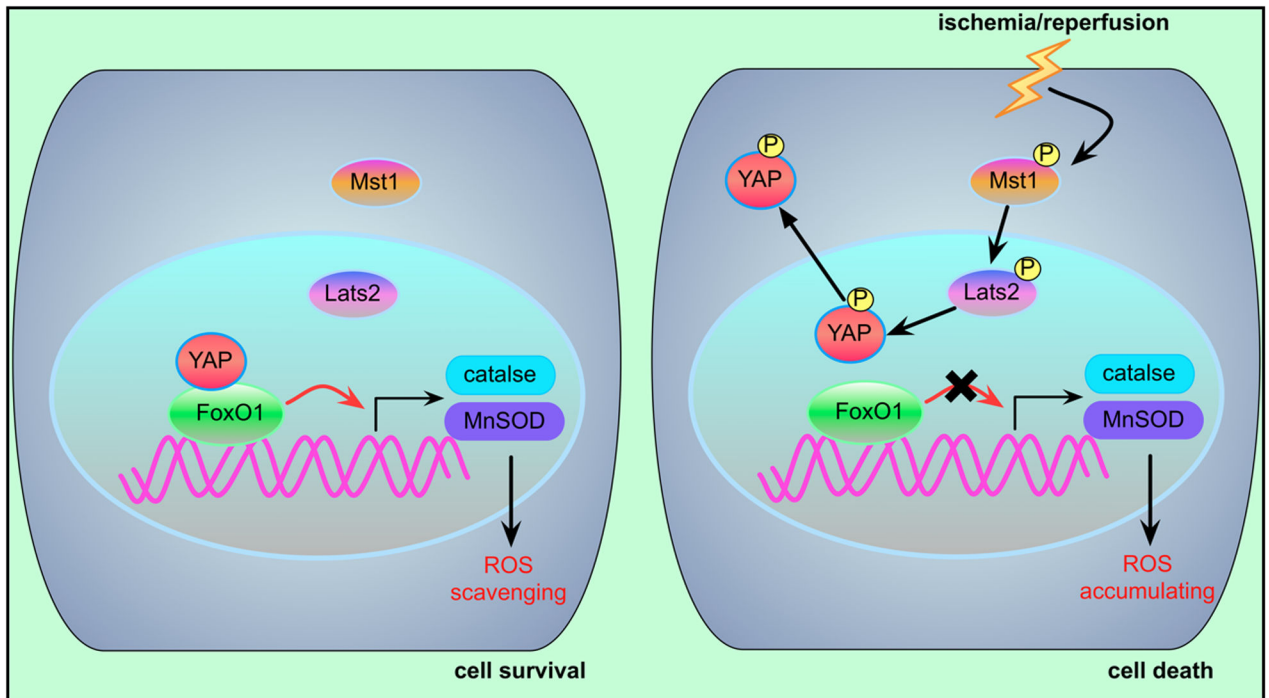


Figure 6. A scheme of the crosstalk between Hippo signaling and FoxO1

In cardiomyocytes, YAP and FoxO1 form a functional complex that mediates catalase and MnSOD expression. In response to I/R, activation of the Hippo signaling cascade induces YAP inactivation, which leads to antioxidant gene suppression, ROS accumulation, and cell death.